Available online at www.sciencedirect.com
ScienceDirect
Journal of Power Sources 171 (2007) 1054–1061
JOURNAL OF POWER SOURCES
www.elsevier.com/locate/jpowsour

The electrochemical capacitance of nanoporous carbons in aqueous and ionic liquids

Hongtao Liu [a,b,*], Guoyi Zhu [a]

[a] *State Key Laboratory of Electroanalytical Chemistry, Changchun Institute of Applied Chemistry, Chinese Academy of Sciences, Changchun 130022, PR China*
[b] *Department of Chemistry and Biochemistry, New Mexico State University, Las Cruces, NM 88003-8001, USA*

Received 28 April 2007; received in revised form 18 June 2007; accepted 19 June 2007
Available online 30 June 2007

Abstract

The electrochemical capacitance of porous carbon materials including activated carbon, carbon nanotubes, and carbon gels were investigated. Due to their different porous structures, these carbons showed different capacitive behaviors in aqueous solutions and ionic liquids. It was found that carbon nanotubes, having the largest micropore volume, and the carbon gels with 3D macroporous framework presented the opposite results in charge capacity in the two media. The experimental data showed that microporous materials presented the higher capacitance in aqueous solutions, while macropores were more favorable for improving power and energy properties in ionic liquids owing to the higher operable voltage of the ionic liquids. This may imply that the capacitive performance of a porous material depends more on its matching degree to the applied electrolytes than on its overall pore volume. Carbon materials with ample macropores could be more suitable to be used in ionic liquids to fully exert the energy output for a capacitor. An electrochemical capacitor based on 3D macroporous carbon gels in ionic liquids has been demonstrated to show a specific energy of 58 W h kg^{-1}, comparable to a commercial battery.

Keywords: Capacitance; Porous carbon; Electrochemical capacitor; Energy performance; Ionic liquid

1. Introduction

Carbon materials have attracted increasing interest over the past years due to their variety of forms and microtextures with unique properties for practical applications. Additionally, many porous carbons are low cost and environmentally friendly materials, and are very promising for electrochemical applications, especially for energy storage. In view of their large specific surface area and low mass density, the study and development of carbon-based electrode materials for electrochemical capacitors has been an important issue in recent years [1–10].

Among these carbon materials, activated carbons are the most attractive electrode materials for electrochemical capacitors from a commercial point of view. They can be derived from charcoals (e.g. wood and coconut), which are conveniently available from nature. In addition, an activated carbon electrode with exceptionally high surface area and well-dispersed pore size distribution can easily accumulate a significant amount of charge at the electric double layer.

Carbon nanotubes were recently discovered [11] and have already shown many novelties in the field of nanosciences [12–16], electronics [17–20], optics [21–24], and functional materials [25–28]. An ideal carbon nanotube can be considered as a hexagonal network of graphene-sheet that has been rolled up to make a seamless hollow cylinder. The special tubular pores with unique electrical properties make carbon nanotubes potential electrode materials for electrochemical capacitors.

Carbon gels are 3D-network porous materials. Concerning their pore structures, micropores are related to the intra-particle structure, whereas mesopores and macropores are produced by the inter-particle structure [29]. Carbon gels are generally

* Corresponding author at: Department of Chemistry and Biochemistry, New Mexico State University, Las Cruces, NM 88003-8001, USA.
Tel.: +1 505 646 4628.
E-mail address: liuht@nmsu.edu (H. Liu).

0378-7753/$ – see front matter © 2007 Elsevier B.V. All rights reserved.
doi:10.1016/j.jpowsour.2007.06.200

obtained by the carbonization of organic gels, which are synthesized by the sol–gel procedure from the polycondensation of different organic monomers. The pore structure of carbon gels can be finely tuned via the adjustment of reactant ratios, curing time, and drying temperature. Therefore, carbon gels can be viewed as very promising porous electrode materials for electrochemical capacitors.

The electrochemical capacitance of a carbon electrode is highly linked to the surface area, the pore size distribution, the ionic accessibility of the electrode material, and the electrolyte properties. In particular, the compatibility of the carbon electrode material with the electrolyte plays the most important role since the electric double layer is built at the electrode/electrolyte interfacial region. The matching of movable electrolyte ions with the pore structure would possibly provide the best capacitor performance having both a large charge capacity and a high power and energy density.

Aqueous electrolytes used in electrochemical capacitors are mostly composed of small inorganic anions and simple hydrated cations (angstrom level) that are easy to access to micropores (1–2 nm) and mesopores (2–50 nm) under the induction of an electric field. Thus, most of the high surface area materials reveal large charge capacity in aqueous electrolyte media. In this regard, aqueous electrolytes seem to be most favorable for pairing with porous materials for electrochemical capacitors. However, due to the low decomposition voltage limit of aqueous solvents (less than 1.2 V), it remains a challenge to achieve a high-performance electrochemical capacitor in aqueous media that are extremely hard to support the higher energy ($E_{max} = 1/2\,CU^2$) output [30].

Ionic liquids have recently become very popular as green solvents applied in synthesis of materials [31–35], catalysis and sensors [36–40], extraction and separation [41–45], and electrochemical processes [46–50]. Ionic liquids possess many novel specialties. Besides their wide range of fluid (~300 °C), ionic liquids have negligible vapor pressure even at elevated temperatures, high ionic conductivity rised up to 0.1 S cm^{-1} [51], excellent thermal and chemical stability, and high heat capacity and cohesive energy density. Compared with commonly employed organic compounds, ionic liquids are less toxic and they are nonflammable. Furthermore, ionic liquids can be strategically designed by alternation of anions or the alkyl groups of cations for each particular application. Also, it should be emphasized that ionic liquids themselves possess large intrinsic capacitance [52] and wide voltage windows (even up to 6.0 V) [53], which makes them the right electrolytes for achieving high-energy electrochemical capacitors.

In this work, we aimed to investigate the electrochemical capacitance of several representative porous carbon materials including activated carbon, carbon nanotubes, and carbon gels in aqueous and ionic liquids. Due to their different porous structures, these materials showed evident differences in the capacitive behaviors in aqueous solutions and ionic liquids. Furthermore, the rank list according to their capabilities in aqueous solutions was inconsistent with that in ionic liquids. This implies that a potentially good capacitive material in one medium is not necessarily efficient in another electrolyte. Therefore, an objective evaluation for a material according to its capacitive properties should be closely associated with the matched electrolyte. In this work, the used carbon gels having the poorest capacitance as a capacitor material in aqueous solution however just revealed a battery-level energy performance (i.e. 58 W h kg^{-1}) in ionic liquids.

2. Experimental

2.1. Pretreatment of ionic liquid

1-Butyl-3-methylimidazolium hexafluorophosphate (BMIM-PF_6, ≥98%, Solvent Innovation) ionic liquid was further purified before use. The purchased BMIM-PF_6 was fully washed with double-deionized water under vigorous agitation. After repeated wash the separated lower-layer organic phase became pale-yellow, while the pH of the settled upper-layer aqueous phase was ca. 7. The organic phase was extracted and then dried in a vacuum box at 100 °C for 24 h. The treated BMIM-PF_6 was in airtight store for later use.

2.2. Treatments and preparation of materials

The commercially activated carbons (particle size: 5–10 um) specifically for the electrochemical capacitor provided by Ningde Xinsen Chemical & Industry Co., Ltd. are received without further treatment. The carbon nanotubes (length: 1–2 um, diameter: 5–10 nm) from Shenzhen Nanotech Port Co., Ltd. was treated as follows. The carbon nanotubes were first oxidized at 400 °C in air for 4 h. To eliminate metal oxide catalysts, the oxidized carbon nanotubes were then dispersed in 6.0 M HCl for 6 h under vigorous agitation, washed with double-deionized water until the pH of the solution was ca. 7. Finally, such treated carbon nanotubes were dried in a vacuum box at 100 °C for 24 h. The carbon gels were prepared through a sol–gel process according to the method proposed by Pekala et al. [54,55]. Resorcinol (R), formaldehyde (F), Na_2CO_3 catalyst (C), and double-deionized water (W) were mixed (molar ratios are: R/F = 0.5, R/W = 0.04, R/C = 1000) under magnetic stirring at room temperature, and then transferred into a glass vial (20 mL). The vial was sealed and kept in sequence at room temperature for 24 h, 50 °C for 36 h, 75 °C for 48 h, 90 °C for 48 h. After being cured, the wet RF organic gels were immersed in acetone for 48 h in order to fully exchange water trapped inside the pores. Then, a freeze-drying treatment was performed by immersing the vial in liquid nitrogen and connecting it to a vacuum pump. By using this freeze-drying method, the solvent was frozen and then removed by sublimation, thereby avoiding the formation of a vapor–liquid interface. The RF gels prepared by this method have a well-developed meso- and macropore network. Finally, the dried RF gels were heated to 800 °C at a heating rate of 10 °C min^{-1} and kept at this carbonization temperature for 5 h under a nitrogen gas flow (600 mL min^{-1}).

The carbon materials used in this paper are referred as AC (activate carbon), CNT (carbon nanotube), MC (a 1:1 mixture of AC and CNT), and CG (carbon gel), respectively.

2.3. Characterization and measurements

The BET specific surface areas and pore volumes of the carbon materials were determined by N_2 gas adsorption at 77 K on a Quantachrome NOVA 1000 (Ver. 6.11) system. The Barrett–Joyner–Halenda (BJH) average pore diameter was calculated by using a NOVA Enhanced Data Reduction Software (Ver. 2.13). The SEM measurements were conducted with a XL30 ESEM FEG scanning electron microscopy at an accelerating voltage of 20 kV. The electrochemical measurements were performed in a three-electrode setup connected to a CHI660 electrochemical work-station. The working electrodes were prepared by mixing the investigated carbon materials with conducting graphite and 5% PTFE binder in a mortar with a ratio of 80:10:10 by weight. The mixtures were then rolled out on foam nickels, pressed at 2 Mpa cm^{-2} to form slices with the thickness of 0.1–0.3 mm. A graphite disk with large area was used as the counter electrode. A Ag/AgCl (in saturated KCl) and a Ag/Ag^+ (10 mM $AgNO_3$ in CH_3CN) pairs were used as the reference electrode in 2 M KCl aqueous solutions and solvent-free ionic liquid electrolytes, respectively. The cyclic voltammetric data were collected between −0.9 and 0.1 V at a scan rate of 50 mV s^{-1} in aqueous solutions, and between −2.0 and 1.0 V at a scan rate of 5 mV s^{-1} in ionic liquid electrolytes. The AC impedance spectra were recorded from 10^5 to 10^{-2} Hz under open circuit condition. The amplitude of the used perturbation was 10 mV. The galvanostatic charge–discharge tests were performed at a current of 500 mA g^{-1} between −0.9 and 0.1 V in aqueous solutions, and of 200 mA g^{-1} between −2.0 and 1.0 V in ionic liquids.

3. Results and discussion

3.1. The pore properties of the carbon materials

Fig. 1 shows the N_2 adsorption–desorption isotherms of various porous carbons. It can be seen that all of the three carbon materials present obvious mesoporous characteristics of type IV with a hysteresis loop at the high relative pressure ($P/P_0 > 0.45$) which is attributed to the capillary condensation of N_2 in mesopores or potential macropores [56]. These carbon materials have their own typical porous textures. In the case of the AC, it is approximately H1 adsorption behavior that the N_2 adsorption amount rockets with the increase of the relative pressure around the $P/P_0 = 0.6$. This implies that there is abundant large-size mesopores within the AC material. The CNT shows a typical H4-type hysteresis loop that is relatively flat. The thin tubular or narrow slotted holes generally produce that loop in the N_2 adsorption–desorption isotherm at the relatively high pressure [57]. The as-prepared CG generates a quasi-H2 hysteresis loop at the very high pressure nearby $P/P_0 = 1$, which reveals an evidently large mesopore and/or potential macropore characteristic within its structure. These findings illustrate that the three representative carbon materials have remarkably different nanopore constructions distributed in the substrate frameworks.

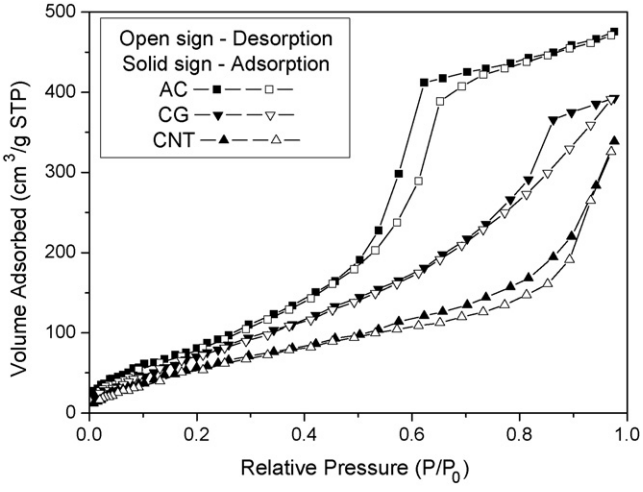

Fig. 1. N_2 adsorption–desorption isotherms of various nanoporous carbons.

The characteristic pore properties of the investigated carbons are listed in Table 1. The highest BET surface area of the AC is responsible for maximum N_2 adsorption total volume. The pore size distribution of the AC is mainly between mesopores and macropores that occupy more than 85% of the total pore volume. One can predict that such constructed AC would be a good electrode material especially for a high-performance electrochemical capacitor. On the contrary, the CNT has the lowest BET surface area and minimum pore size. The majority of its pores are between mesopores and micropores. In lack of large-sized pores, it is possible that it will not suitable for application to organic electrolyte systems. The CG is patterned with large-sized mesopores and overwhelming macropores that would very possibly endow this material with novel properties matched with big organic electrolyte ions. These hypotheses will be electrochemically proven later.

Fig. 2 shows the surface morphologies of the investigated porous carbon materials. The AC is composed of the aggregates of carbon slices and terraces. The large-sized mesopores and macropores are formed between the aggregates, and the small-sized mesopores and micropores are built from the curved slices within the aggregates. Large quantities of the smaller pores contribute to a higher BET surface area, while the existed larger pores effectively improve the compatibility of the capacitive material with electrolyte. The inter-tangled fine tubular carbons construct the CNT network, and the hole size is almost comparative or smaller to the tube diameter. The as-constituted CNT structure has a relatively high ratio of micropores and small-sized mesopores. The MC material is fabricated by full-scale grinding the mixture of the AC and the CNT with 1:1 (by weight). It seems that the mechanical force does not untangle the nanotube network. However, the carbon aggregates of the AC have been loosen, and some carbon particles are dispersed into the CNT network and reconstructed a layer framework. The as-prepared CG is evidently different from the other carbon materials observed from the surface morphology. It is a 3D porous hard-substrate carbon structure. The walls of the structure are not smooth which is advantageous for the adsorption of the charged species from the electrolyte solution. Meanwhile, the

Table 1
Characteristic pore properties of the representative carbons

Carbon material	S_{BET} ($m^2\ g^{-1}$)	D_{mean} (nm)	V_{micro} ($cm^3\ g^{-1}$)	V_{meso} ($cm^3\ g^{-1}$)	V_{macro} ($cm^3\ g^{-1}$)	V_{total} ($cm^3\ g^{-1}$)
AC	1500	47.3	0.11	0.34	0.28	0.73
CNT	260	6.2	0.13	0.25	0.07	0.45
CG	770	73.7	0.07	0.12	0.47	0.66

S_{BET}: BET surface area; D_{mean}: mean pore diameter; V_{micro}: volume of micropore (<2 nm); V_{meso}: volume of mesopore (2–50 nm); V_{macro}: volume of macropore (>50 nm); V_{total}: total pore volume.

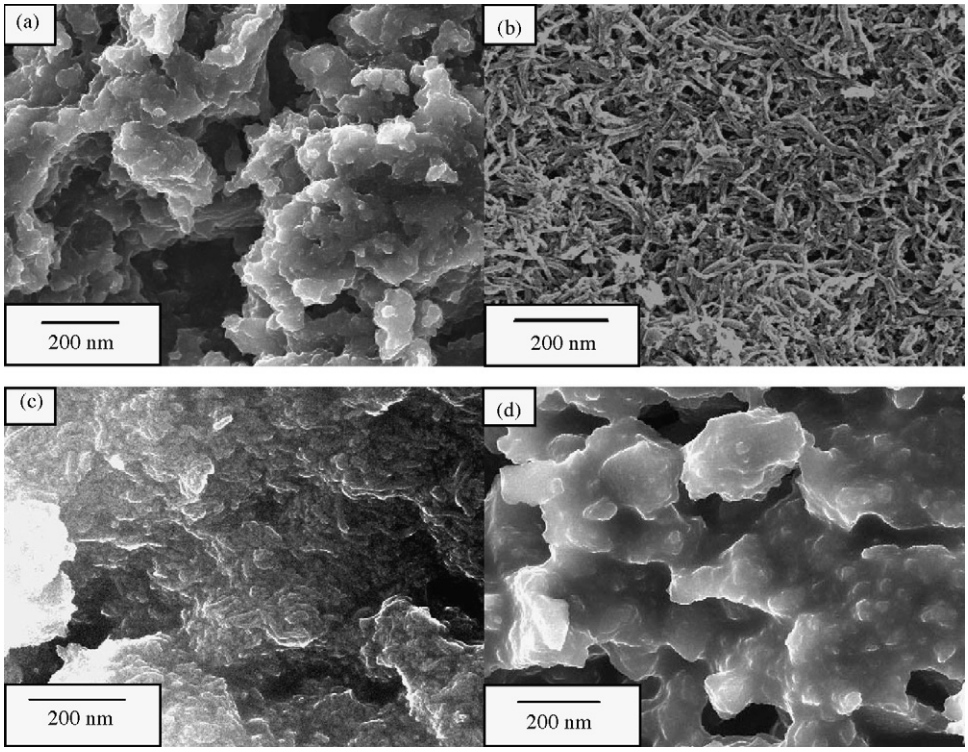

Fig. 2. Surface morphologies of the investigated carbon materials: (a) AC, (b) CNT, (c) MC, (d) CG.

larger 3D pores surrounded by the carbon walls afford facilities for the transportation of big ions. Therefore, the as-prepared CG is theoretically more advantageous when used as the electrode material in big organic ions electrolytes for a high-performance electrochemical capacitor.

3.2. The electrochemical capacitance of the carbon materials in aqueous solutions

Fig. 3 shows the cyclic voltammograms of the investigated porous carbons in 2 M KCl aqueous solutions. There exist small faradaic redox waves in the 1 V potential windows, which give rise to pseudocapacitance. Generally, the commercial carbon materials contain rich sp^2-bonded surface functional groups that are unsaturated and highly active. Under the stimulation of an electric field, these active groups easily combine with OH^- and Cl^- of aqueous solutions via the addition or substitution interactions and result into irreversible faradaic reactions. But the irreversible reactions would weaken with the continuous cyclic voltammetric process that increase the amount of carbon atoms saturated. Therefore, the surface-active groups play the roles of

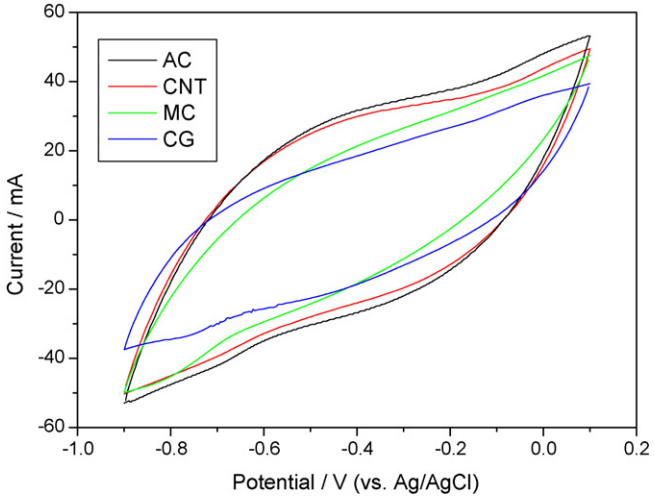

Fig. 3. Cyclic voltammograms of the investigated nanoporous carbons in 2 M KCl aqueous solutions at a scan rate of 50 mV s^{-1} between −0.9 and 0.1 V.

enhancing the electrochemical capacitance only during the first several charge–discharge cycles.

From the cyclic voltammograms in Fig. 3, it is observed that the AC and the CNT present relatively larger pseudocapacitance than the other carbons due to their richer surface groups. As regards the MC, it does not present as much pseudocapacitance as either the AC or the CNT individually does, although it is entirely composed of the AC and the CNT. This may as well be ascribed to the reassembled surface carbon structures under the mechanical force during the full-scale grinding process. The as-prepared GC synthesized by a sol–gel process does not generate the unsaturated carbons and therefore has less pseudocapacitance.

The largest electrochemical capacitance of the AC in the aqueous solutions is mainly due to its highest BET surface area as well as richer surface-active groups. However, the CNT having the least BET surface area contributes to a large electrochemical capacitance in the aqueous solutions. This should be closely associated with its microstructures. By comparing the data listed in Table 1, it is easy to find that the AC has the maximum volume of micropores. Micropores are more competitive than big pores for small inorganic ions exchanging charges with the carbon substrates because of their adjacent distances. Therefore the high ratio of micropores is favorable to enhance the electrochemical capacitance of the material in the aqueous solutions. The decrease of the capacitance for the MC is mainly originated from part of carbon particles dispersed into the CNT network, which reduce the available pore space. Contrary to the CNT, the GC shows relatively less electrochemical capacitance in the aqueous solution due to its high ratio of macropores increasing the resistance of charge exchange.

The electrochemical impedance behaviors of the investigated nanoporous carbons in the aqueous solutions are shown in Fig. 4. The small arcs that appeared at mid-high frequencies imply that there are small charge-transfer resistances between the electrodes and the electrolytes for these carbon materials matching with the aqueous electrolytes. The linear slopes at low frequencies reflect the electrochemical capacitive characteristics of various carbon electrode materials. The steeper and the closer to the imaginary axis the plot is, the purer and the larger the capacitance is. Obviously, the AC and the CNT show a good capacitive performance in the aqueous solutions in which the capacitive lines are more ascendant with the decreasing frequencies. However, the GC does not reveal the ideal capacitive behavior in the aqueous solutions where it only has a relatively moderate slope. The outcomes from the impedance profiles are in agreement with those from the cyclic voltammograms.

3.3. The electrochemical capacitance of the carbon materials in ionic liquids

The big organic and inorganic ions of the ionic liquid are unable to move as fast as the small inorganic ions of the aqueous solutions. It is therefore necessary to carry out relatively slow cyclic voltammetry to probe the electrochemical capacitance in the ionic liquid.

Fig. 5 shows the cyclic voltammograms of the investigated nanoporous carbons in BMIM-PF_6 ionic liquids at a scan rate of 5 mV s^{-1} between −2.0 and 1.0 V. It can be seen that there are not apparent pseudocapacitance for these carbons in the ionic liquids. This is possibly because the ionic liquids themselves have relatively large intrinsic capacitance [52] that may cover the inconspicuous faradaic current waves. Interestingly, the CG and the CNT display opposite capacitive behaviors in the ionic liquids and the aqueous solutions. The CG due to its 3D marcoporous structures gives the maximum electrochemical capacitance in the ionic liquids while the CNT having the higher electrochemical capacitance in the aqueous solutions only presents the least in the ionic liquids. Ionic liquids are composed entirely of large ions and ion pairs and therefore are hard to move in or out of micropores. Although the CNT has the highest ratios of micropore volumes, the accessible pores within it for the ionic liquids are relatively low, and that causes a reduction of its effective adsorption volume. This finding implies that

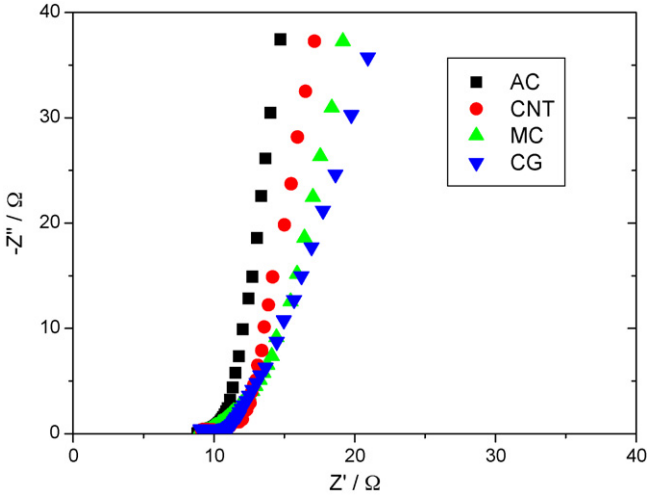

Fig. 4. Electrochemical impedance behaviors of the investigated nanoporous carbons in the aqueous solutions with a perturbation amplitude of 10 mV from 10^5 to 10^{-2} Hz under open circuit condition.

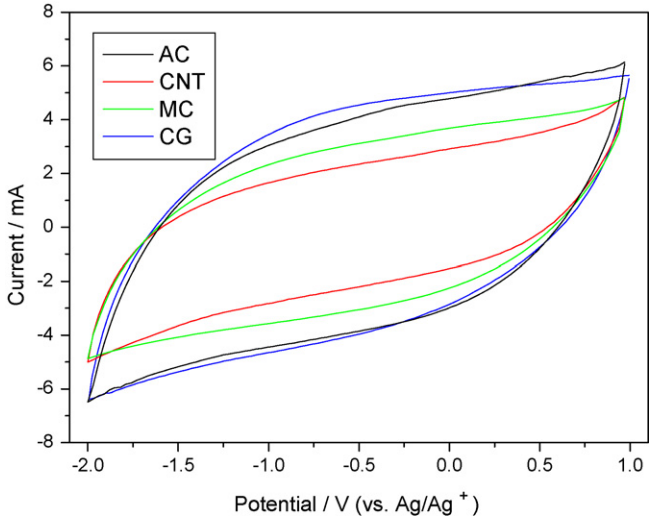

Fig. 5. Cyclic voltammograms of the investigated nanoporous carbons in BMIM-PF_6 ionic liquids at a scan rate of 5 mV s^{-1} between −2.0 and 1.0 V.

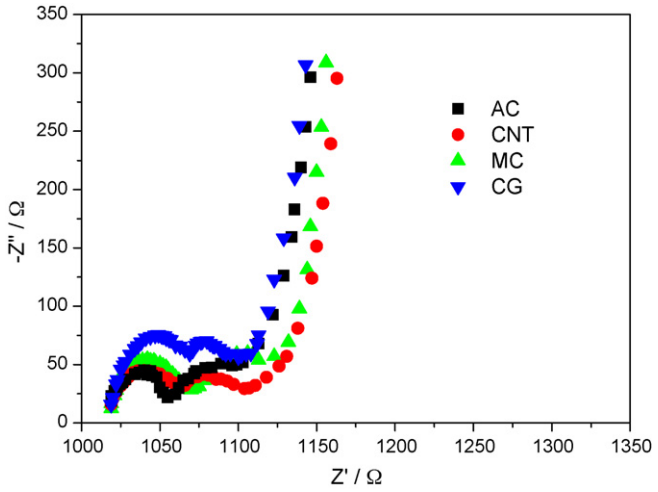

Fig. 6. Electrochemical impedance behaviors of the investigated nanoporous carbons in BMIM-PF_6 ionic liquids with a perturbation amplitude of 10 mV from 10^5 to 10^{-2} Hz under open circuit condition.

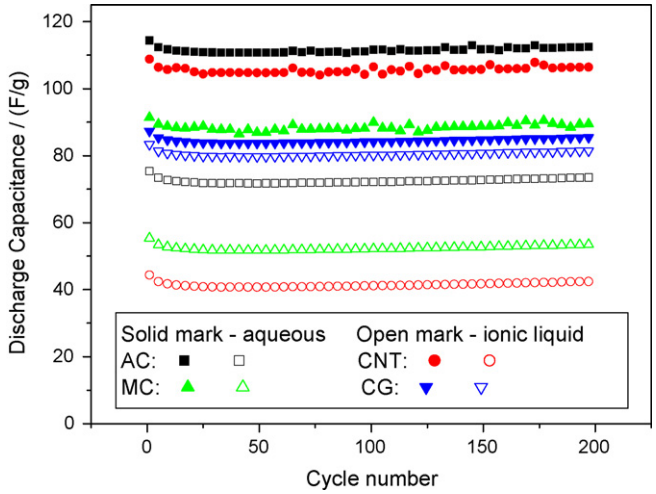

Fig. 7. Charge–discharge performance of the nanoporous carbons during 200 cycles with the charge–discharge current of 500 mA g^{-1} in the aqueous solutions and 200 mA g^{-1} in the ionic liquids, respectively.

the capacitance for a material depends more on its matchable pores to the electrolytes than on its overall pore volume.

The electrochemical impedance also illustrates that these nanoporous carbons have quite different capacitive behavior in the ionic liquids from that in the aqueous solutions. Shown in Fig. 6, besides the whole capacitive lines at low frequencies are more vertical, there are two apparent arcs at mid-high frequencies in the ionic liquids. In the aqueous solutions, the small charge carriers are effortless to directly access to the surface pores of a material under an electrical field. The overall electrode processes are determined by the exchange of charges between the ions of the pores and the electrons of the electrode material. Thus, there is only one RC time constant for this process, i.e. expressing one arc at the electrochemical impedance profile.

However, the big ions and ion pairs of the ionic liquids are difficult to access to the surface pores of a material because of their giant size and clumsy mobility. Additionally, the charge-transfer process between the ionic liquids and the electrode is not fast enough. Therefore the overall electrode processes in the ionic liquids depend on both mass transport and charge exchange. The two RC time constants are responded to two arcs at the impedance profile. The dimension of the arc reflects the reaction rate of the corresponding process. It is obvious that the electrode kinetics in the ionic liquids is far slower than that in the aqueous solution. However, the almost vertical capacitive lines at low frequencies illustrate the capacitance performance in the ionic liquids is more stable than that in the aqueous solutions. The capacitance outcomes for these carbon materials obtained from the electrochemical impedance data are quite consistent with those from the cyclic voltammetries.

3.4. The charge–discharge performance of the carbon materials

To further verify the above analyses, these nanoporous carbon materials are measured by means of a galvanostatic charge–discharge technique. The applied currents for the aqueous solutions and the ionic liquid system are 500 and 200 mA g^{-1}, respectively.

Shown in Fig. 7 is the charge–discharge performance of the carbon materials during 200 cycles. At the first several cycles (before the tenth), the discharge capacity is a little bit more than the followings due to the irreversible faradaic pseudocapacitance. As the cycles increase, the capacity tends to be invariable. The mean coulombic efficiencies for these carbon materials are more than 98% in the aqueous solutions and 99.5% in the ionic liquids, which illustrate that these nanoporous carbons can be used as electrochemical capacitor materials. The key performance data are summarized in Table 2.

Although the capacitance for most of the nanoporous carbons in the ionic liquids is evidently less than that in the aqueous solutions, the as-prepared CG presents almost the same value in both

Table 2
Key data from the charge–discharge of the investigated carbon materials

Carbon material	Aqueous			Ionic liquid		
	C_m (F g^{-1})	P_{max} (W kg^{-1})	E_{max} (W h kg^{-1})	C_m (F g^{-1})	P_{max} (W kg^{-1})	E_{max} (W h kg^{-1})
AC	114	1155	7.1	75	452	52
CNT	108	992	6.4	44	307	26
MC	91	1008	6.3	55	443	48
CG	87	1226	6.7	83	516	58

C_m: specific capacitance; P_{max}: maximum specific power; E_{max}: maximum specific energy.

media. This can be ascribed to the unchangeable effective pore space for the macroporous material in various electrolytes. The result also reveals that the capacitance of the macroporous material is less dependent on the used electrolyte. The specific powers for these carbon materials in the ionic liquids are not comparable with those in the aqueous solutions because of the relatively higher electrochemical resistances of the formers. However, the electrochemical capacitors based on these carbon materials in the ionic liquids still have the powers (300–500 W kg^{-1}) far higher than the common batteries. One of the most valuable properties of the ionic liquids is the wide operable electrochemical potential that provides the high work voltage. Therefore, these nanoporous carbons paired with the ionic liquids exhibit extremely high-energy densities. The electrochemical capacitor based on the macroporous CG in the ionic liquids even shows a specific energy of 58 W h kg^{-1} that is comparable to the commercial alkaline battery. These thrilling outcomes confirm that the electrochemical capacitors based on the ionic liquid electrolytes can not only act as the supporting power sources assisting the high-performance batteries, but also individually serve as the main power sources replacing the low-power neutral or alkaline batteries.

4. Conclusions

The electrochemical capacitance of several nanoporous carbons has been investigated considering their different pore characteristics. It is found that these carbon materials have quite different capacitive behaviors in the aqueous solutions and in the ionic liquids. The CNT having maximum micropore volume and the as-prepared CG with a 3D macroporous framework present entirely opposite charge capacity in the two electrolytes, which illustrate that the microporous materials have a higher capacitance in the aqueous solution while the macropores are more favorable for the ionic liquids. This implies that the capacitance for a material relies more on its compatibility with the electrolytes than its overall pore volume. Although the electrode kinetics in the ionic liquids is far slower than that in the aqueous solutions because of the relatively higher electrochemical resistance for the former, the energy performance in the ionic liquids is far superior to that in the aqueous solution owing to the high operable voltage of the ionic liquids. The electrochemical capacitor based on the macroporous CG in the ionic liquids even shows a specific energy of 58 W h kg^{-1}, comparable to the commercial battery. Therefore it is hopeful to replace the low-power batteries containing unwholesome additives with the high-energy electrochemical capacitors based on environmentally friendly ionic liquids.

Acknowledgements

This work was financially supported by the National 863 Program (No. 2002AA601330) of China. The authors gratefully acknowledge Professor Cynthia G. Zoski and Doctor Jose L. Fernandez of New Mexico State University for their key points to this work.

References

[1] S. Yoon, J.W. Lee, T. Hyeon, S.M. Oh, J. Electrochem. Soc. 147 (2000) 2507–2512.
[2] E. Frackowiak, F. Beguin, Carbon 39 (2001) 937–950.
[3] C.S. Li, D.Z. Wang, J.J. Wu, W.Z. Lu, J. Liang, J. Inorg. Mater. 18 (2003) 1010–1016.
[4] Q.H. Meng, L. Liu, H.H. Song, R. Zhang, L.C. Ling, J. Inorg. Mater. 19 (2004) 593–598.
[5] X.F. Wang, Chin. J. Electron. 14 (2005) 45–48.
[6] H. Tamai, M. Kunihiro, M. Morita, H. Yasuda, J. Mater. Sci. 40 (2005) 3703–3707.
[7] G.H. Yuan, Z.H. Jiang, A. Aramata, Y.Z. Gao, Carbon 43 (2005) 2913–2917.
[8] Y.Z. Wei, B. Fang, S. Iwasa, M. Kumagai, J. Power Sources 141 (2005) 386–391.
[9] K. Okajima, A. Ikeda, K. Kamoshita, M. Sudoh, Electrochim. Acta 51 (2005) 972–977.
[10] J. Li, X.Y. Wang, Q.H. Huang, S. Gamboa, P.J. Sebastian, J. Power Sources 158 (2006) 784–788.
[11] S. Iijima, Nature 354 (1991) 56–58.
[12] M. Wilson, Nano Lett. 4 (2004) 299–302.
[13] T. Wang, M. Wang, X. Hu, X. Qu, F. Zhao, S. Dong, Langmuir 21 (2005) 12068–12071.
[14] Y.C. Xing, J. Phys. Chem. B 108 (2004) 19255–19259.
[15] B. Yi, R. Rajagopalan, H.C. Foley, U.J. Kim, X.M. Liu, P.C. Eklund, J. Am. Chem. Soc. 128 (2006) 11307–11313.
[16] J. Chen, C.H. Xue, R. Ramasubramaniam, H.Y. Liu, Carbon 44 (2006) 2142–2146.
[17] T. Yamada, Appl. Phys. Lett. 78 (2001) 1739–1741.
[18] J.Q. Wei, H.W. Zhu, B. Jiang, L.J. Ci, D.H. Wu, Carbon 41 (2003) 2495–2500.
[19] M.L. Usrey, E.S. Lippmann, M.S. Strano, J. Am. Chem. Soc. 127 (2005) 16129–16135.
[20] E. Bekyarova, M.E. Itkis, N. Cabrera, B. Zhao, A.P. Yu, J.B. Gao, J. Am. Chem. Soc. 127 (2005) 5990–5995.
[21] H. Kuzmany, W. Plank, M. Hulman, C. Kramberger, A. Gruneis, T. Pichler, Eur. Phys. J. B 22 (2001) 307–320.
[22] S.Y. Set, H. Yaguchi, Y. Tanaka, M. Jablonski, J. Lightwave Technol. 22 (2004) 51–56.
[23] A. Hartschuh, H.N. Pedrosa, J. Peterson, L. Huang, P. Anger, H. Qian, ChemPhysChem 6 (2005) 577–582.
[24] J.H. Mun, S.W. Kim, J. Kor. Phys. Soc. 48 (2006) L175–L177.
[25] S. Joseph, R.J. Mashl, E. Jakobsson, N.R. Aluru, Nano Lett. 3 (2003) 1399–1403.
[26] W.H. Lee, S.J. Kim, W.J. Lee, J.G. Lee, R.C. Haddon, P.J. Reucroft, Appl. Surf. Sci. 181 (2001) 121–127.
[27] A.M. Benito, W.K. Maser, M.T. Martinez, Inter. J. Nanotech. 2 (2005) 71–89.
[28] T.I.T. Okpalugo, P. Papakonstantinou, H. Murphy, J. McLaughlin, N.M.D. Brown, Carbon 43 (2005) 153–161.
[29] N. Yoshizawa, H. Hatori, Y. Soneda, Y. Hanzawa, K. Kaneko, M.S. Dresselhaus, J. Non-Cryst. Solids 330 (2003) 99–105.
[30] B.E. Conway, Electrochemical Supercapacitors: Scientific Fundamentals and Technological Applications, Kluwer Academic/Plenum Publishers, New York, 1999, pp. 259–297.
[31] Y. Zhou, M. Antonietti, J. Am. Chem. Soc. 125 (2003) 14960–14961.
[32] S.V. More, S.S. Ardhapure, N.H. Naik, S.R. Bhusare, W.N. Jadhav, R.P. Pawar, Synth. Commun. 35 (2005) 3113–3118.
[33] L.X. Yang, Y.J. Zhu, W.W. Wang, H. Tong, M.L. Ruan, J. Phys. Chem. B 110 (2006) 6609–6614.
[34] H.G. Zhu, J.F. Huang, Z.W. Pan, S. Dai, Chem. Mater. 18 (2006) 4473–4477.
[35] Y. Liu, J.J. Peng, S.R. Zhai, J.Y. Li, J.J. Mao, M.J. Li, Eur. J. Inorg. Chem. (2006) 2947–2949.
[36] C.P. Mehnert, R.A. Cook, N.C. Dispenziere, E.J. Mozeleski, Polyhedron 23 (2004) 2679–2688.
[37] B.C. Ranu, R. Jana, Adv. Syn. Catal. 347 (2005) 1811–1818.

[38] Y. Liu, L.H. Shi, M.J. Wang, Z.Y. Li, H.T. Liu, J.H. Li, Green Chem. 7 (2005) 655–658.
[39] H.T. Liu, P. He, Z.Y. Li, C.Y. Sun, L.H. Shi, Y. Liu, Electrochem. Commun. 7 (2005) 1357–1363.
[40] Z.Y. Li, Q. Zhang, H.T. Liu, P. He, X.D. Xu, J.H. Li, J. Power Sources 158 (2006) 103–109.
[41] J.G. Huddleston, H.D. Willauer, R.P. Swatloski, A.E. Visser, R.D. Rogers, Chem. Commun. (1998) 1765–1766.
[42] A.E. Visser, R.P. Swatloski, S.T. Griffin, D.H. Hartman, R.D. Rogers, Sep. Sci. Tech. 36 (2001) 785–804.
[43] T. Nakashima, T. Kawai, Chem. Commun. (2005) 1643–1645.
[44] H.L. Huang, H.P. Wang, G.T. Wei, I.W. Sun, J.F. Huang, Y.W. Yang, Environ. Sci. Tech. 40 (2006) 4761–4764.
[45] C.Y. He, S.H. Li, H.W. Liu, K. Li, F. Liu, J. Chromatogr. A 1082 (2005) 143–149.
[46] P. He, H.T. Liu, Z.Y. Li, Y. Liu, X.D. Xu, J.H. Li, Langmuir 20 (2004) 10260–10267.
[47] P. He, H.T. Liu, Z.Y. Li, J.H. Li, J. Electrochem. Soc. 152 (2005) E146–E153.
[48] Z.Y. Li, H.T. Liu, Y. Liu, P. He, J.H. Li, J. Phys. Chem. B 108 (2004) 17512–17518.
[49] Z.Y. Li, H.T. Liu, Y. Liu, P. He, J. Li, L.Z. Zheng, Polymer 46 (2005) 7578–7584.
[50] H.T. Liu, P. He, Z.Y. Li, Y. Liu, J.H. Li, Electrochim. Acta 51 (2006) 1925–1931.
[51] R. Hagiwara, T. Hirashige, T. Tsuda, Y. Ito, J. Electrochem. Soc. 149 (2002) D1–D6.
[52] H.T. Liu, P. He, Z.Y. Li, Y. Liu, J. Li, L.Z. Zheng, Electrochem. Solid-State Lett. 8 (2005) J17–J19.
[53] T. Sato, G. Masuda, K. Takagi, Electrochim. Acta 49 (2004) 3603–3611.
[54] R.W. Pekala, J. Mater. Sci. 24 (1989), 3221-2277.
[55] R.W. Pekala, C.T. Alviso, F.M. Kong, S.S. Hulsey, J. Non-Cryst. Solids 145 (1992) 90–98.
[56] S. Shiraishi, H. Kurihara, L. Shi, T. Nakayama, A. Oya, J. Electrochem. Soc. 149 (2002) A855–A861.
[57] K.S.W. Sing, D.H. Everett, R.A.W. Haul, L. Moscou, P.A. Pierotti, J. Rouquerol, Pure Appl. Chem. 57 (1985) 603–619.